JOURNAL OF GEOPHYSICAL RESEARCH, VOL. 86, NO. B7, PAGES 6155–6169, JULY 10, 1981

# Stress Diffusion Along Rupturing Plate Boundaries

F. K. LEHNER, V. C. LI, AND J. R. RICE

*Division of Engineering, Brown University, Providence, Rhode Island 02912*

An analysis is made of viscoelastic lithosphere/asthenosphere coupling in the time-dependent redistribution of stress along plate boundaries or other seismic lineaments following great earthquakes. The study is based on a generalization by Rice of Elsasser's model of stress-diffusion, in which general elastic plane stress deformations are allowed in lithospheric plates which are coupled in an elementary way to a (Maxwellian) viscoelastic asthenosphere. Solutions are developed which describe the large-scale quasi-static distribution of thickness-averaged stresses in the lithosphere at or near stationary or travelling rupture zones, modeled here by either crack-like zones of fixed stress drop or dislocation-type slip zones. Sudden ruptures shed load onto the asthenosphere which is gradually transferred back to the lithosphere by a slow relaxation process. The spatial and temporal characteristics of the predicted stress alterations suggest a significant role of lithosphere/asthenosphere coupling effects in triggering interactions of great earthquakes, patterns of prolonged aftershock activity, and the breaking of barriers or gaps by time-dependent stressing.

## INTRODUCTION

We are concerned in this study with long-term processes by which great earthquake ruptures transfer stress laterally to neighboring sections of a plate boundary or other seismic lineaments, and with the effect of such time-dependent stress redistribution on the triggering of further ruptures. Indeed, the questions as to the triggering mechanism and, related to it, the repeat time of great earthquakes seem to be viewed in distinctly different ways depending on the emphasis placed by a particular model on one or another aspect of the phenomenon. For example, modern versions of *Reid*'s [1910] elastic rebound hypothesis have been developed in the form of essentially two-dimensional models of strike slip faulting in which the fault extends vertically downwards from the Earth's surface to some depth in a lithospheric plate, viscoelastic and freely sliding in the model of *Budiansky and Amazigo* [1976] or, more realistically, elastic and dynamically coupled to a semi-infinite viscoelastic substrate in the models of *Nur and Mavko* [1974], *Savage and Prescott* [1978*a*, *b*], *Spence and Turcotte* [1979], and *Turcotte et al.* [1979].

As shown first by Budiansky and Amazigo, such models are capable of exhibiting an infinite sequence of earthquake cycles (pre-earthquake strain accumulation, co-seismic strain release, and post-seismic readjustment). Typically, when the shear stress has risen to the critical level of a static shearing resistance along the fault plane, the strain accumulated while the fault was locked is released by sudden relative slip across the fault to an extent corresponding to a drop in stress to some lower value of (dynamic) shearing resistance. The load which, according to the more complete models, is thereby suddenly placed on an asthenospheric substrate will be relaxed there gradually due to the assumed viscoelastic response while tectonic loading associated with plate motion will renew the preseismic accumulation of strain along the fault and lead into the next earthquake cycle.

Two-dimensional models of the type just described, in which conditions remain essentially uniform along strike, could be quite unrealistic (unless reinterpreted as representative of locally uniform near-fault conditions) if earthquake ruptures are triggered primarily in response to disturbances arising from inhomogeneities along the strike of a seismic lineament. Indeed, the case has been made repeatedly in the past for the propagation of triggering effects and the current broader interest in this question is reflected, for example, in a large number of studies devoted to the seismic gap problem (see, e.g., *Wyss* [1979]). Also, *Brune* [1979] has recently discussed the significance for earthquake prediction based on premonitory phenomena of propagating triggering effects. Brune has argued that such effects might in fact invalidate any attempt to predict an earthquake from observations of premonitory signals, in part simply by the absence of such signals prior to the arrival of the trigger. This indeed would seem to be a possible defect of the above-discussed models. However, as shown by an analysis of regional events prior to the 1976 Haicheng earthquake [*Scholz*, 1977], a travelling 'deformation front,' as Scholz has called it, may be viewed as a critical premonitory signal, accessible to observation and obviously worth a closer study.

Support of the idea of propagation of earthquake triggering disturbances along tectonic lineaments comes from observations of seismic migration patterns along plate boundaries [*Fedotov*, 1965; *Mogi*, 1968*a*, *b*; *Kelleher*, 1970; *Sykes*, 1971; *Delsemme and Smith*, 1979], the classic example being furnished by the North Anatolian fault in Turkey [*Richter*, 1958; *Mogi*, 1968*a*; *Ambraseys*, 1970; *Dewey*, 1976; *Toksöz et al.*, 1979]. In the case of the North Anatolian fault a clear trend of westward migration appears for earthquakes above magnitude 7, commencing with the great Eastern Anatolian earthquake of 1939. The mode of propagation is one in which successive ruptures, extending up to 200 km in length, abut rather than overlap, while exhibiting an average rate of migration of about 80 km/yr. Several observations on the North Anatolian fault zone appear consistent with migration patterns of seismic activity observed along the circum-Pacific belt. Thus, for example, in the northwestern circum-Pacific, *Fedotov* [1965] and *Mogi* [1968*b*] have identified a sequential occurrence of great shallow earthquakes in which the seismic belt was nearly continuously covered by aftershock areas without significant overlap. Mogi estimates migration speeds between 150 and 270 km/yr. for these events (although consecutive earthquakes in the series considered do not generally form a stepwise continuous progression of rupture but, rather, often leave gaps which are subsequently filled). The inferred speeds are of the same order as the approximately 100 km/yr. of the 'deformation front' which presumably triggered the Haicheng earthquake [*Scholz*, 1977]. There appears to be some evidence, on



Paper number 1B0490.
0148-0227/81/001B-0490$01.00

the other hand, in support of a speculation expressed by *Wood and Allen* [1973] in a study of seismic migrations along the San Andreas fault that migration speeds may vary with magnitude of seismic events, a conjecture based on a comparison of their own findings of a south-north migration at 3 km/yr of events $M \geq 5.0$ with data discussed by *Savage* [1971] which suggest a south-north migration at 60 km/yr for events $M \geq 7.2$.

*Savage* [1971] and *Ida* [1974] have developed theories of propagating disturbances aiming at an explanation of observed seismic migration patterns. In these theories the constitutive response of fault gouge material enters as the rate determining factor.

Here we wish to focus on a larger scale aspect of migrating seismicity and deal with the subject of stress transfer along plate boundaries, allowing for stationary as well as for travelling disturbances as the primary sources of stress alteration. We take up an idea suggested by *Bott and Dean* [1973] and pursued more explicitly by *Anderson* [1975] according to which certain global scale similarities between seismic migration patterns ought to be interpreted as manifestations of stress diffusion in an elastic lithosphere riding over a viscous asthenosphere as in *Elsasser*'s [1969] theory of lithospheric stress guides. This idea seems indeed supported by Anderson's first estimates of seismicity migration speeds. It would therefore appear highly desirable to pursue further a theory of stress diffusion, similar in spirit to Elsasser's, but free of principal shortcomings of the latter associated with the assumption of a purely viscous response of the asthenosphere and with consideration only of deformations that propagate in a single direction. Hence in this paper we present an analysis of great earthquake disturbances on the basis of a plate theory proposed by *Rice* [1980], which generalizes Elsasser's by allowing for general plane stress deformation states in elastic lithospheric plates and for a Maxwellian viscoelastic behavior of an asthenospheric substrate, as is essential for more realistic modeling of time-dependent stress alterations at rupturing plate boundaries. Large scale effects of viscoelastic relaxation, which may be expected to play a role during time spans of the order of repeat times for great earthquakes, are thereby made amenable to the relatively simple analysis afforded by a two-dimensional plate/foundation model.

## THEORY

### *Propagation of Deformation in an Elastic Plate Overlying a Viscoelastic Foundation*

We now present a simple model of a linearly elastic lithospheric plate of uniform thickness $H$ riding on a viscoelastic asthenosphere, as developed previously by *Rice* [1980]. Our interest is directed towards horizontally propagating deformations created by and spreading out from large scale ruptures along a plate boundary.

If $\sigma_{\alpha\beta}$ ($\alpha, \beta = x, y$) are the thickness averaged stresses in the plane of the plate, the exact equations of equilibrium are

$$\partial\sigma_{\alpha\beta}/\partial x_\alpha = \tau_\beta/H \tag{1}$$

where $\tau_\beta$ is the shearing traction acting on the lower surface of the plate in the negative $\beta$-direction. Here and subsequently, summation over the values $x, y$ is implied by repeated Greek indices. Letting $u_\alpha$ be the thickness averaged displacements in the plane of the plate, the stress-strain relations for an isotropic material are

$$\sigma_{\alpha\beta} = G\left[\frac{\partial u_\alpha}{\partial x_\beta} + \frac{\partial u_\beta}{\partial x_\alpha} + \frac{2\nu}{1-\nu}\frac{\partial u_\gamma}{\partial x_\gamma}\delta_{\alpha\beta}\right] \tag{2}$$

under plane stress conditions, where $G$ is the shear modulus and $\nu$ is the Poisson ratio. The plane stress model applies when the average stress disturbance in the thickness direction is negligible in comparison with the in-plane components, and this should be appropriate for disturbances of dominant wavelengths that are comparable to or greater than $H$ (e.g., great earthquakes).

We treat interactions with the asthenosphere in the spirit of the simple Elsasser model, but generalize it to that of a linear Maxwell body (elastic and viscous element in series). First, for the cases when elastic response can be neglected we write, following Elsasser,

$$\tau_\alpha = \eta\dot{u}_\alpha/h \tag{3}$$

and observe that this should be accurate especially if, as is widely suspected, the asthenosphere consists of a zone having a thickness $h$ of the same order as $H$, but a viscosity $\eta$ very much lower than that of adjoining material. Otherwise, we simply regard $\eta/h$ as some effective coupling parameter obtained by matching model predictions to observed diffusion of deformation. The incorporation of elastic effects through a similar model is less suitable but in the interest of simplicity we use the Maxwell generalization

$$\dot{\tau}_\alpha b/G + \tau_\alpha h/\eta = \dot{u}_\alpha \tag{4}$$

where $b$ is an effective length for short-time elastic coupling. Later we shall suggest that if the elastic constants are regarded as uniform through the lithosphere and asthenosphere, an appropriate choice of $b$ is

$$b = (\pi/4)^2 H \tag{5}$$

On the other hand, if the suspected layer $h$ below the lithosphere had a (quasi-static) shear modulus $G_1$ much smaller than $G$, it would be appropriate to write

$$b = hG/G_1 \tag{6}$$

Probably, the most suitable value is a little larger than the greater of these two estimates.

When the equilibrium, stress-strain, and Maxwell coupling equations are combined there results

$$\left(\alpha + \beta\frac{\partial}{\partial t}\right)\left\{\frac{\partial^2 u_\gamma}{\partial x_\rho \partial x_\rho} + \frac{1+\nu}{1-\nu}\frac{\partial^2 u_\rho}{\partial x_\gamma \partial x_\rho}\right\} = \frac{\partial u_\gamma}{\partial t} \tag{7}$$

$$\alpha \equiv hHG/\eta \qquad \beta \equiv bH$$

These equations for $u_\gamma$ are, in fact, too complicated to solve in closed form for all but the simplest boundary value problems and shortly we will introduce a physically motivated model equation which has solutions that agree with those of the general equations in some important limiting cases. However, the nature of the deformations predicted by the general equations can be somewhat clarified by isolating the equations satisfied by the dilation $\varepsilon$ and rotation $\omega$, where

$$\varepsilon = \partial u_x/\partial x + \partial u_y/\partial y \qquad 2\omega = \partial u_y/\partial x - \partial u_x/\partial y \tag{8}$$

One finds that these satisfy uncoupled differential equations

$$\begin{aligned}(\alpha + \beta\partial/\partial t)\nabla^2\varepsilon &= [(1-\nu)/2]\partial\varepsilon/\partial t \\ (\alpha + \beta\partial/\partial t)\nabla^2\omega &= \partial\omega/\partial t\end{aligned} \tag{9}$$

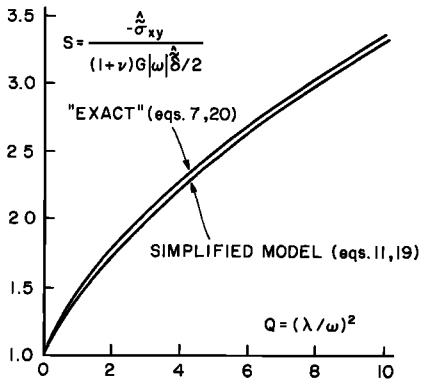


Fig. 1. Amplitude factor $S$ for Fourier-Laplace transformed stress $\hat{\sigma}_{xy}$ on plate boundary in response to general slip distribution $\delta(x, t)$.

with $\nabla^2 = \partial^2/\partial x^2 + \partial^2/\partial y^2$. In the case when elastic coupling effects are neglected ($\beta = 0$) these are classical diffusion equations, and it is seen that $\alpha$ and $2\alpha/(1 - \nu)$ are the respective diffusivities for propagation of rotation and dilation. Thus, for Elsasser's problem of a long portion of plate boundary suddenly relieved of stress, the appropriate diffusivity is $\alpha$ for the strike-slip mode along a transform fault, and $2\alpha/(1 - \nu)$ for the compressive mode on a shallow thrust fault.

For very long faults, exact solutions to (7) or (9) for constant stress drop or slip displacement boundary conditions along the fault may be obtained without difficulty and were given previously by *Rice* [1980] in a first analysis of the present plate model. When a more general situation obtains, such as with faults of finite length, closed form solutions to (7) or (9) are difficult to find. For disturbances created along seismic zones of large linear extent progress can be made, however, through analysis of a simplified model which we shall now discuss.

*Simplified Plate Equations for the Analysis of Transfer of Stress and Deformation Along Plate Boundaries*

We shall now introduce a model, based on a simplification of (7), which will be more amenable to analysis than the latter while furnishing approximations good enough for problems involving the transfer of disturbances along seismic zones of large linear extent.

To fix ideas, we focus on the case of a long transform boundary coinciding with the $x$ direction in the plate, letting $u$ be the dominant displacement component $u_x$. Further, we treat the plate as if it were constrained in the $y$ direction, ignoring the displacement and equilibrium equations for that direction. A closer match to the actual plate behavior can be obtained by not using the $x$ component of (7) with $u_y$ set to zero but, rather, by beginning anew with equilibrium and stress-strain relations in the form

$$\partial\sigma_{xx}/\partial x + \partial\sigma_{xy}/\partial y = \tau_x/H$$
$$\sigma_{xx} = M\partial u/\partial x \qquad \sigma_{xy} = G\partial u/\partial y \tag{10}$$

Here $M$ is an effective modulus that we choose as $(1 + \nu)^2 G$ because, as we show, this allows the simple model to simulate exactly the relation of the more general model between slip and shear stress drop for arbitrary slip distributions along the plate boundary, in the important limiting case for which the foundation is completely relaxed ($\tau_\beta = 0$). Thus when $\tau_x$ is related to $u$ as in the Maxwell model of (4), the governing equation is

$$\left(\alpha + \beta\frac{\partial}{\partial t}\right)\left\{(1 + \nu)^2\frac{\partial^2 u}{\partial x^2} + \frac{\partial^2 u}{\partial y^2}\right\} = \frac{\partial u}{\partial t} \tag{11}$$

which is of the same character as (7), (9) for the more general model.

We now consider the accuracy of the model represented by (11). First, in the limit of long wavelength disturbances ($\partial^2 u/\partial x^2$ negligible), as for nearly uniform stress drops along very long segments of the plate boundary (i.e., Elsasser's problem, but with Maxwell coupling) the more general equations (7) reduce to exactly the same equation for $u(= u_x)$. Also, if we examine the relaxed limit $\tau_x = 0$, equivalent to setting time derivatives in (11) equal to zero, and consider two joined semi-infinite plates with an arbitrary distribution of slip $\delta(x)$ along their boundary, where

$$\delta(x) = u(x, y = 0^+) - u(x, y = 0^-) \tag{12}$$

it is elementary to verify that the solution to (11) is

$$u(x, y) = -\frac{1}{2\pi}\int_{-\infty}^{+\infty}\frac{d\delta(x')}{dx'}\arctan\left[\frac{(1 + \nu)y}{x - x'}\right]dx' \tag{13}$$

where $-\pi \le \arctan \le +\pi$. This leads to shear stresses along the fault given by the Cauchy principal value integral

$$\sigma_{xy}(x, 0) = G\frac{\partial u}{\partial y}(x, 0) = -\frac{(1 + \nu)G}{2\pi}\int_{-\infty}^{+\infty}\frac{d\delta(x')/dx'}{x - x'}dx' \tag{14}$$

As remarked, we have chosen $M$ to make this equation agree with the exact solution to the full elastic plane stress equations (e.g., see *Bilby and Eshelby* [1968] or *Rice* [1968]; these references actually give the result analogous to (14) for plane strain, in which $(1 + \nu)$ of (14) is replaced by $1/(1 - \nu)$, but as noted in the latter reference this is just the transformation which converts a plane stress solution to a plane strain solution). A consequence of this last result is, for example, that in the case of a shear crack with some prescribed distribution of stress drop along its length, in the relaxed limit both the simple model and the exact plane stress solution give the same distribution of $\delta(x)$ along the fault and the same intensification of shear stress $\sigma_{xy}(x, 0)$ outside it. Finally, because the foundation response is irrelevant in the limit of short wavelength disturbances (at least when $\beta \neq 0$), the simple and the more general model give identical responses along the fault plane in that limit also.

The accuracy of the simple model of (11) in general may be addressed in a more abstract manner by taking Fourier and Laplace transforms of $u$:

$$\tilde{u}(\omega, y, t) = \int_{-\infty}^{+\infty} u(x, y, t)e^{-i\omega x}\,dx$$
$$\hat{\tilde{u}}(\omega, y, s) = \int_0^{\infty}\tilde{u}(\omega, y, t)e^{-st}\,dt \tag{15}$$

The transformed solution of (11) corresponding to an arbitrary slip history $\delta(x, t)$ for $t > 0$ is then

$$\hat{\tilde{u}} = (y/2|y|)\hat{\tilde{\delta}}\exp\{-(1 + \nu)(\omega^2 + \lambda^2)^{1/2}|y|\} \tag{16}$$

where

$$\lambda^2 = s/[(1 + \nu)^2(\alpha + \beta s)] \tag{17}$$

The resulting transformed shear stress on $y = 0$ is

$$\hat{\tilde{\sigma}}_{xy} = -(1 + \nu)G|\omega|S\hat{\tilde{\delta}}/2 \tag{18}$$

where the amplitude factor $S$ (normalized to $S = 1$ in the relaxed state) is

$$S = (1 + Q)^{1/2} \tag{19}$$

with $Q = (\lambda/\omega)^2$. The solution to the 'exact' equations (7) for this problem is derived in Appendix A and when the resulting expression for $\hat{\sigma}_{xy}$ is written in the form of (18) above, one finds

$$S = \frac{[2/(1-\nu)^2 + Q]^2 - [4/(1+\nu)^2][1/(1+\nu)^2 + Q]^{1/2}[1/(1+\nu)^2 + (1-\nu)Q/2]^{1/2}}{Q[1/(1+\nu)^2 + Q]^{1/2}} \tag{20}$$

For $Q = 0$ this $S = 1$ and for large $Q$ it behaves as $Q^{1/2}$, just as for (19) above. The two results for $S$ are compared in Figure 1, for the case $\nu = 0.25$, and they are seen to agree closely over the full range of $\omega$ and $S$. Hence, in view of the complexity of (20) as compared with (19), we limit all further consideration to the simplified model and expect that negligible inaccuracies will result from this.

To see the origin of the estimate of $b$ (and hence $\beta$, since $\beta = bH$) given in (5) we observe that for sudden loadings the asthenosphere reacts elastically, with $\tau_x = Gu/b$ in our model, and (11) reduces to

$$\beta[(1+\nu)^2\partial^2 u/\partial x^2 + \partial^2 u/\partial y^2] = u \tag{21}$$

for the short time thickness average displacements of the lithosphere. If we suppose that a very long segment of the plate boundary suddenly undergoes a stress drop $q$, the resulting solution for $u$ is

$$u = (q\beta^{1/2}/G)e^{-y/\beta^{1/2}} \tag{22}$$

for $y > 0$. By comparison, the anti-plane strain elasticity solution for a very long strike slip type discontinuity, sustaining a stress drop $q$ uniformly through the lithosphere thickness $H$, is

$$u(y, z) = (q/G)\ \mathrm{Im}\ \{[(z + iy)^2 - H^2]^{1/2} - (z + iy)\} \tag{23}$$

Here $u(y, z)$ is the local (versus thickness average) displacement, the $z$ axis is directed downward with $z = 0$ at the Earth's surface (left-sensed coordinate system), and the square root has its branch cut along $-H < z < H$. The corresponding thickness average displacement at $y = 0^+$ is

$$\frac{1}{H}\int_0^H u(0^+, z)\,dz = \frac{\pi}{4}\frac{q}{G}H \tag{24}$$

and comparison with (22) suggests that we choose

$$\beta^{1/2} = (\pi/4)H \tag{25}$$

which is the origin of the estimate of $b$ given in (5).

A weakness of the representation of short time elastic response within the model is, however, that the resulting exponential decay of $u$ with $y$ is more rapid than the $1/y^2$ decay based on the anti-plane elasticity solution. Thickness average displacements calculated from (22) and (23) are compared in Figure 2. We emphasize, however, that if the considerations leading to the estimate of $b$ in (6) are valid (i.e., $G_1$ much less than $G$), then our manner of incorporating elastic coupling with the asthenosphere is more realistic and (22) is likely to be in better agreement than suggested by Figure 2 with the (unknown) precise solution of the elasticity equations analogous to (23).

We note that a simplified equation similar to (11) can be written when the $x$ axis defines a line of plate convergence and faulting takes place as low angle thrusting in a subduction zone. In a two-dimensional plate model the dominant displacement component now becomes $v \equiv u_y$ and stress drops are associated with the component $\sigma_{yy}$. When the $x$ direction is regarded as constrained, so that we ignore displacements and equilibrium requirements in that direction, the governing equations are

$$\begin{aligned} &\partial\sigma_{xy}/\partial x + \partial\sigma_{yy}/\partial y = \tau_y/H \\ &\sigma_{xy} = N\partial v/\partial x \qquad \sigma_{yy} = [2G/(1-\nu)]\partial v/\partial y \end{aligned} \tag{26}$$

Here $2G/(1-\nu)$ is the modulus consistent with (2) and the effective modulus $N$ is chosen as $G(1+\nu)^2(1-\nu)/2$ to ensure the same relation between displacement $v$ along the fault and drops in stress $\sigma_{yy}$ as for the exact plane stress model of (7) in the relaxed limit. Thus, (4) and (26) give

$$\left(\alpha + \beta\frac{\partial}{\partial t}\right)\left\{(1+\nu)^2\frac{1-\nu}{2}\frac{\partial^2 v}{\partial x^2} + \frac{2}{1-\nu}\frac{\partial^2 v}{\partial y^2}\right\} = \frac{\partial v}{\partial t} \tag{27}$$

and this agrees with the more general model also in the long wavelength limit, corresponding to Elsasser boundary conditions of uniform stress drop over a long portion of the plate boundary [*Rice*, 1980]. For very long ruptures the dominant deformation modes predicted by (11) and (27) are simple shearing and uniaxial stretching, respectively. According to what has been said earlier, the propagation of deformation into the plate away from the ruptured boundary will be governed in each of these cases by a characteristic diffusivity, namely, $\alpha$ for the shearing mode and $2/(1-\nu) \approx 3\alpha$ for the stretching, i.e., dilational mode.

We observe that if a particular solution of (11) for the strike-slip mode is

$$u = f(x, y, t)$$

then a corresponding solution to (27) for the thrust mode is given by

$$v = f\{[2/(1-\nu)]^{1/2}x, [(1-\nu)/2]^{1/2}y, t\}$$

or by any constant times this expression. We shall develop all subsequent solutions for the strike-slip mode, but reinterpret

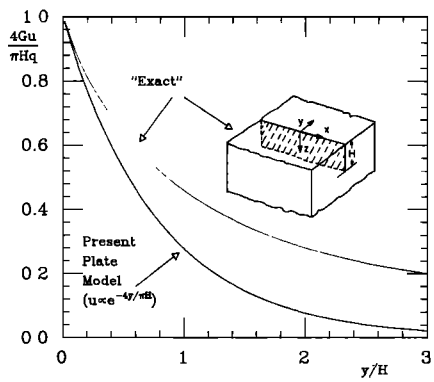


Fig. 2. Decay with distance from fault of thickness averaged displacements as predicted by plate model and by 'exact' elasticity solution for uniform stress drop $q$ over $H$, assuming no variation of elastic properties with depth.

results in terms of the above transformation as needed to discuss the thrust mode.

Finally, we must specify numerical values for the parameters $\alpha$ and $\beta$ so as to provide an interpretation of subsequent results. Selecting $b$ as given by (5) we have $\beta = (H\pi/4)^2$ and therefore $\beta/\alpha = (\pi/4)^2 H\eta/hG$ for the relaxation time of the Maxwell foundation. We shall assume $G = 5.5. \times 10^{10}$ Pa for the mean shear modulus of the crust and upper mantle. An appropriate choice of viscosity $\eta$ is uncertain and, indeed, if the linear model adopted here is to simulate approximately what is an inherently non-linear viscous response of the asthenosphere [e.g., *Melosh*, 1976], different choices of $\eta$ may be appropriate according to the application [*Rudnicki*, 1980]. We have chosen to base numerical illustrations here on the value $\eta = 2.0 \times 10^{19}$ Pa s ($2.0 \times 10^{20}$ poise). This value is consistent with the characteristic time $2\eta/G = 20$ yr. obtained in recent work by *Thatcher et al.* [1980] on earthquake loading data, if the above $G$ is used. (Thatcher et al. infer $\eta = 1.0 \times 10^{19}$ Pa s from this data, since they choose $G = 3.0 \times 10^{10}$ Pa as the mean shear modulus of a 30 km thick elastic plate.) The chosen value, $\eta = 2 \times 10^{19}$ Pa s, falls into the range of $5 \times 10^{18}$ Pa s to $5 \times 10^{19}$ Pa s set by earlier inferences of *Nur and Mavko* [1974] from earthquake loading data and *Walcott* [1973] from the isostatic rebound of Lake Bonneville. Furthermore, we shall assume $H = 75$ km for the thickness of the elastic layer (lithosphere) and $h = 100$ km for the thickness of the viscoelastic substrate (asthenosphere), taking note that only the ratio $H/h$ enters into the relaxation time, the value of which is thus $\beta/\alpha = 4.6$ yr. For convenience we use the value $\beta/\alpha \approx 5$ yr in the following. Further, the dependence of the time scale of results on the value chosen for viscosity is discussed when appropriate subsequently.

## Time-Dependent Stress Alterations Associated With Sudden Ruptures

A first question arising within the framework of our model concerns the time-dependent stressing of a plate boundary in the vicinity of or directly on segments that have failed in a sudden great earthquake rupture event. Two simple and in a sense complementary models of such faulting are analyzed in this section. In the first the fault is idealized as a crack-like zone of sudden and permanent stress drop while in the second model the rupture is viewed as a suddenly introduced zone of slippage, represented by a fixed dislocation density distribution. It should be recalled that stress-drop and slippage here refer to thickness-averaged quantities; we do not at this point examine variations of stress or slip through the lithospheric thickness.

The crack model and the dislocation model furnish two extremes in terms of actual time-dependent response. In fact, in each a certain readjustment (of stress and slip displacement, respectively) is suppressed which may be expected for any natural fault plane from material behavior such as time-dependent strengthening of frictional contact surfaces and creep. It seems likely, however, that the somewhat more realistic rupture model is that of the second kind, in which fault slippage associated with a suddenly formed crack is kept at its initial value and the resulting dislocation-type problem is analyzed, as is done in the second part of this section.

### *The Suddenly Introduced Crack*

Consider first the problem of a suddenly introduced zone of stress drop covering some segment of a transform fault and modeled here as a crack-like zone of slippage which reaches down to the base of the elastic plate. We will assume here that slippage is resisted along the crack faces by a stress $\tau_F$ which, in accordance with our plane stress model, must be viewed as an average taken over the plate thickness. In a complete description of the process, which we do not attempt here, $\tau_F$ would contain contributions corresponding to frictional sliding of brittle rock in the upper sections of the plate and from perhaps quasi-plastic slip at greater depths, where pressure and temperature are higher.

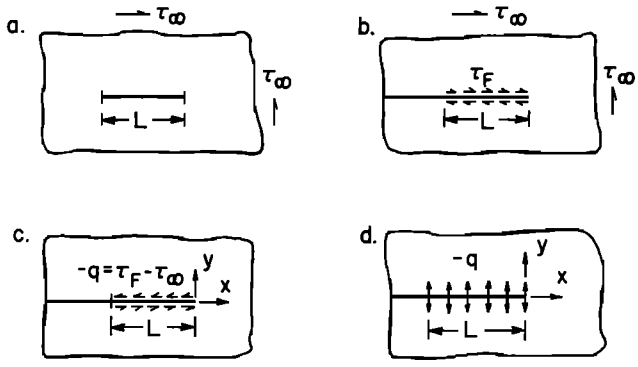


Fig. 3. Definition of crack problems for strike-slip (Figures 3*a*–3*c*) and thrust faulting (Figure 3*d*) modes of rupture on transform and subduction type plate boundary, respectively.

As shown in Figure 3*a*, the zone of active slippage is viewed in a horizontal plane like a shear crack of length $L$ loaded in Mode II by a remotely uniform shear stress $\tau_\infty$. However, in order to simplify the subsequent analysis, we shall in fact deal with the case of a semi-infinite zone of slippage, indicated in Figure 3*b*, the strength of which is reduced to a level $\tau_F$ over a certain distance $L$ extending behind the 'crack tip.' *Rice and Simons* [1976] observe that this approximation of Figure 3*a* by Figure 3*b* involves little error and, in fact, corresponds to a certain amount of entrapped slip in the fault of Figure 3*a*. Subtracting out the uniform tectonic stress $\tau_\infty$, the problem then becomes one in which a 'stress drop' $\tau_\infty - \tau_F$ occurs along a segment of length $L$ along the crack focus with the sense shown in Figure 3*c*, i.e., such that the half planes $y \gtrless 0$ experience the same relative displacement as for the original loading of Figure 3*b*. Finally, in Figure 3*d* is shown a plan view of the corresponding Mode I (thrust) problem for a subduction-type plate boundary.

The shear crack problem of Figure 3*c* possesses anti-symmetry, implying

$$u(x, y, t) = -u(x, -y, t) \tag{28}$$

We are thus led to a boundary value problem for (11), subject to the subsidiary conditions

$$\begin{aligned} &u(x, y, 0) = 0 && \\ &u(x, 0, t) = 0 && x > 0 \\ &G\partial u/\partial y(x, 0, t) = -q(x)H(t) && x < 0 \\ &\partial u/\partial x, \partial u/\partial y \to 0 && x^2 + y^2 \to \infty \end{aligned} \tag{29}$$

where $H(\cdots)$ is the unit step function. The loading conditions of Figure 3*c* correspond to $q(x) = qH(x + L)$, where $q$ is the constant stress drop $\tau_\infty - \tau_F$. The form of the third condition follows from (10) while the second is a direct consequence of (28). We shall now employ Fourier transform and Wiener-Hopf techniques (see, e.g., *Noble* [1958]) to construct a solution.

Fourier and Laplace transformations of (11) again provide

us with the general solution (16) for the transform $\hat{u}$ The boundary condition $u(x, 0, t) = 0$ for $x > 0$ implies

$$\hat{u}(\omega, 0^+, s) = \frac{1}{2}\hat{\delta}(\omega, s) = \int_{-\infty}^{0} \hat{u}(x, 0^+, s)e^{-i\omega x}\,dx \equiv \hat{U}_+(\omega, s) \tag{30}$$

where the sumbol $\hat{U}_+(\omega, s)$ adopted for the integral means that $\hat{U}_+(\omega, s)$ is analytic in the upper complex $\omega$ plane (Im $(\omega) > 0$), given that the displacement remains bounded everywhere. Similarly, the condition along $x < 0$ leads to

$$G\partial\hat{u}(\omega, 0, s)/\partial y = -Q(\omega)/s + \hat{T}_-(\omega, s) \tag{31}$$

where $Q(\omega)$ is the Fourier transform of the loading

$$Q(\omega) = \int_{-\infty}^{0} q(x)e^{-i\omega x}\,dx \tag{32}$$

which can be assumed to be analytic in the half plane Im $(\omega) > 0$, and

$$\hat{T}_-(\omega, s) = \int_0^{\infty} \hat{\sigma}_{xy}(x, 0, s)e^{-i\omega x}\,dx \tag{33}$$

which is analytic in a half plane Im $(\omega) < \tau$. Here $\tau > 0$ at any finite time denotes the decay index of $\sigma_{xy}(x, 0, t)$, i.e., $\sigma_{xy}(x, 0, t) = O(e^{-\tau x})$ as $x \to +\infty$.

Differentiation of (16) and use of (30) and (31) now furnishes the relation

$$(1 + \nu)G(\omega^2 + \lambda^2)^{1/2}\hat{U}_+(\omega, s) = Q(\omega)/s - \hat{T}_-(\omega, s) \tag{34}$$

valid in a strip of the complex $\omega$ plane, which is delimited by the overlap of the domains of definition of the analytic functions $\hat{U}_+$ and $\hat{T}_-$.

In Appendix B we develop the solution to (34) by standard Wiener-Hopf methods. This is done there by first representing the loading $q(x)$ in the form

$$q(x) = \frac{1}{2\pi}\int_{-\infty}^{\infty} Q(\kappa)e^{i\kappa x}\,d\kappa \tag{35}$$

which is the Fourier inversion of (32). A solution is then constructed for the elementary loading $q(x) = e^{i\kappa x}$, $x < 0$ where $\kappa$ is regarded as having an arbitrarily small but negative imaginary part. The resulting expressions for $\hat{U}_+$ and $\hat{T}_-$ are distinguished by a superscript $(\kappa)$, referring to the particular elementary loading, and are given by (B6) and (B7). Superposition of these elementary solutions, weighted by $(1/2\pi)Q(\kappa)$ in the same manner as for $q(x)$ above, then yields the solutions for general load distributions in the form

$$(1 + \nu)G\hat{\bar{u}}(\omega, 0^+, s) = \frac{i}{2\pi s}\int_{-\infty-i\delta}^{+\infty-i\delta} \frac{Q(\kappa)\,d\kappa}{(\omega - \kappa)(\omega + i\lambda)^{1/2}(\kappa - i\lambda)^{1/2}} \tag{36}$$

for the transform of the crack surface displacement, and

$$\hat{\bar{\sigma}}_{xy}(\omega, 0, s) = \hat{T}_-(\omega, s) - Q(\omega)/s = -\frac{i}{2\pi s}\int_{-\infty-i\delta}^{+\infty-i\delta}\left(\frac{\omega - i\lambda}{\kappa - i\lambda}\right)^{1/2}\frac{Q(\kappa)\,d\kappa}{\omega - \kappa} \tag{37}$$

for the transform of the shear stress.

We shall not attempt to perform the inversions and integrations necessary to obtain $u$ and $\sigma_{xy}$ everywhere. Rather, we focus attention on the most interesting part of the solution which gives the stress straight ahead of the crack tip as well as the displacement behind it. The first is obtained by inverting (37). With (32) determining $Q(\kappa)$, the Fourier inversion theorem gives the result

$$\hat{\sigma}_{xy}(x, 0, s) = -\frac{i}{4\pi^2 s}\int_{-\infty}^{0} q(\xi)\,d\xi \int_{-\infty-i\delta}^{+\infty-i\delta} d\kappa \int_{-\infty}^{+\infty}\left(\frac{\omega - i\lambda}{\kappa - i\lambda}\right)^{1/2}\frac{e^{-i(\kappa\xi - \omega x)}}{\omega - \kappa}\,d\omega \tag{38}$$

An appropriate shift of integration contours permits this to be written as

$$\hat{\sigma}_{xy}(x, 0, s) = \frac{1}{\pi^2 s}\int_{-\infty}^{0} q(\xi)e^{-\lambda(x-\xi)}\,d\xi \int_0^{\infty}\int_0^{\infty}\left(\frac{\rho}{\tau}\right)^{1/2}\frac{e^{-\rho x + \tau\xi}}{\rho - \tau}\,d\rho\,d\tau \tag{39}$$

The double integral in this expression is readily evaluated in terms of known Laplace transforms (see, e.g., *Erdelyi et al.* [1954]). This yields the Laplace transform for the stress ahead of the crack

$$\hat{\sigma}_{xy}(x, 0, s) = \frac{1}{s\pi x^{1/2}}\int_{-\infty}^{0} q(\xi)\frac{(-\xi)^{1/2}}{x - \xi}e^{-\lambda(x-\xi)}\,d\xi \qquad x > 0 \tag{40}$$

for any loading $q(x)$ given on $x < 0$.

A measure of the stress concentration at $x = 0$ is given by the Mode II stress intensity factor, defined by

$$K(t) = \lim_{x \to 0^+}\{(2\pi x)^{1/2}\sigma_{xy}(x, 0, t)\}$$

From (40), upon taking this limit, we find

$$\hat{K}(s) = \frac{1}{s}\left(\frac{2}{\pi}\right)^{1/2}\int_{-\infty}^{0} q(\xi)\frac{e^{\lambda\xi}}{(-\xi)^{1/2}}\,d\xi \tag{41}$$

In the case of a uniform stress drop $q$ occurring over $-L \le x \le 0$

$$\hat{K}(s) = \frac{1}{s}q(2/\lambda)^{1/2}\,\mathrm{erf}\,[(\lambda L)^{1/2}] \tag{42}$$

The Laplace transform inversion of (40) and (41) is achieved with the help of a theorem given in *Carslaw and Jaeger* [1948]. Details are carried out in Appendix C1, the result being

$$\sigma_{xy}(x, 0, t) = \frac{1}{\pi x^{1/2}}\int_{-\infty}^{0} q(\xi)\frac{\mu(x - \xi, t)(-\xi)^{1/2}\,d\xi}{x - \xi} \qquad x > 0 \tag{43}$$

where

$$\mu(x - \xi, t) \equiv e^{-\alpha t/\beta}\int_0^{\infty} e^{-\eta}\,\mathrm{erfc}\,[(x - \xi)\lambda_0/(2\eta^{1/2})] \cdot I_0[2(\eta\alpha t/\beta)^{1/2}]\,d\eta$$

$$\lambda_0 \equiv 1/[(1 + \nu)\beta^{1/2}]$$

Here $I_0(\cdot)$ is a modified Bessel function and $I_0(0) = 1$. Similarly we obtain

$$K(t) = \left(\frac{2}{\pi}\right)^{1/2}\int_{-\infty}^{0} q(\xi)\frac{\mu(-\xi, t)}{-\xi^{1/2}}\,d\xi \tag{44}$$

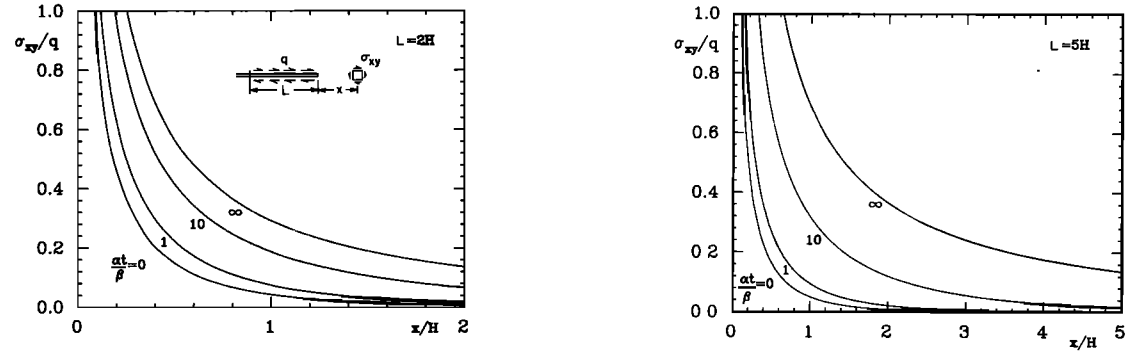


Fig. 4. Stress alteration along transform boundary ahead of suddenly introduced zone of uniform stress drop $q$ (crack model) at various times.

Specialized for a uniform stress drop $q$ occurring over $-L \leq x \leq 0$, these results are appropriately normalized and plotted in Figures 4 and 5 for different times, expressed as multiples of the relaxation time $\beta/\alpha$, as well as for various ratios of rupture length to lithosphere thickness. These solutions represent the transition from an initial stress state characterized by a purely elastic, unrelaxed response of the asthenosphere, to a final state of a completely relaxed asthenosphere exhibiting the known response of an elastic plate with traction-free lower surfaces. Characteristically, as time progresses, the relaxing asthenosphere supports less and less of the load shed onto it initially by the failing lithosphere until ultimately the asthenosphere is completely relaxed and the stress and stress concentration associated with faulting reaches a stationary maximum within the elastic plate. A characteristic time scale for this transfer of stress from newly-ruptured segments of a plate boundary to adjacent potential 'gap zones' thus emerges from our model of lithosphere/asthenosphere coupling and together with predicted magnitudes of stress alterations constitutes a feature of prime interest. We shall further discuss this after presentation of more results.

The behavior of the solutions plotted in Figures 4 and 5 in the unrelaxed ($t \to 0^+$) and completely relaxed ($t \to \infty$) limits is embodied in the following analytical expressions. For $t = 0^+$, i.e., immediately after the coseismic slip,

$$\sigma_{xy}(x, 0) = \frac{q}{\pi x^{1/2}} \int_{-L}^{0} \frac{-\xi^{1/2}}{x - \xi} e^{-(x-\xi)\lambda_0} \, d\xi \qquad x > 0 \qquad (45)$$

which is readily obtained from (40) upon noticing that $\lim_{s\to\infty} \{\lambda(s)\} = 1/[(1 + \nu)\beta^{1/2}] = \lambda_0$. In the completely relaxed limit $t \to \infty$ ($\lambda \to 0$), on the other hand, one has the well-known result

$$\sigma_{xy}(x, 0) = (2q/\pi)(L/x)^{1/2}[1 - (x/L)^{1/2} \arctan (L/x)^{1/2}] \qquad x > 0 \qquad (46)$$

The corresponding results for the stress intensity factor are easily deduced from (42). Thus, in the unrelaxed state, $t \to 0^+$,

$$K = q(2/\lambda_0)^{1/2} \operatorname{erf} (\lambda_0 L)^{1/2} \qquad (47)$$

while for $t \to \infty$

$$K = q(8L/\pi)^{1/2} \qquad (48)$$

which is a familiar result of fracture mechanics. In preparing Figures 4 and 5 we have taken $\nu$ as 0.25 and for simplicity of interpretation have replaced $\lambda_0^{-1} = (1 + \nu)\beta^{1/2} \approx (1 + \nu)\pi H/4 = 0.98H$ by $H$ in all of the relations involved. In particular, the same replacement enables us to write (47) as $K \approx q(2H)^{1/2}$ erf $(L/H)^{1/2}$, so that when $L/H$ is equal to 4 or larger, the initial value of $K$ is effectively independent of $L$ and is given by $K \approx q(2H)^{1/2}$. By comparison, the relaxed value (48) of $K$ has no limit as $L$ increases indefinitely.

An asymptotic result for the stress at $t \gg \beta/\alpha$ is

$$\sigma_{xy}(x, 0, t) = \frac{q}{\pi x^{1/2}} \int_{-L}^{0} \frac{-\xi^{1/2}}{x - \xi} \operatorname{erfc} \left\{ \frac{x - \xi}{2(1 + \nu)(\alpha t)^{1/2}} \right\} d\xi \qquad x > 0 \qquad (49)$$

and a corresponding expression for $K$ may be written down immediately. These asymptotic solutions for times much larger than the relaxation time $\beta/\alpha$ display the behavior of *Elsasser*'s [1969] original model wherein the asthenosphere behaves like a Newtonian viscous fluid. The value of $\beta/\alpha = 5$ yr, however, restricts the usefulness of asymptotic results for $t \gg \beta/\alpha$ and hence also the validity of Elsasser's model quite severely, as is apparent also in Figures 4 and 5 from the time span covered by significant post-seismic stress alterations in response to sudden stress drops.

As is evident from Figure 4, the time scale governing the stress transfer to segments of the plate boundary bordering the rupture zone cannot be characterized simply in terms of the relaxation time $\beta/\alpha$. This slow ascent to the ultimate stress distribution (46) reflects the $1/(t)^{1/2}$ decay at large times of the function $\mu(r + x, t)$ in (43) and is qualitatively similar to the behavior of the model developed by *Thatcher et al.* [1980] in their study of lithospheric loading by dip-slip earthquakes. We shall further comment on stress transients when comparing the crack solution with the dislocation solution below.

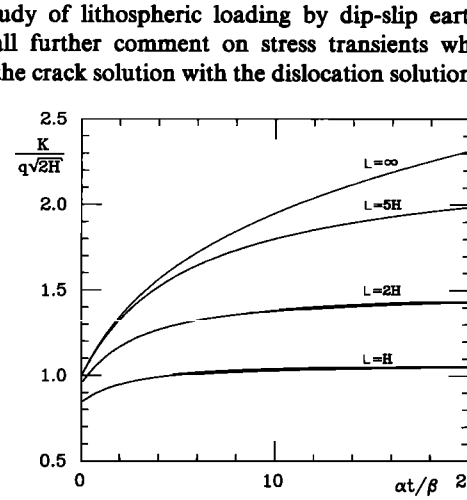


Fig. 5. Thickness average stress intensity factor associated with suddenly introduced zones of permanent stress drop (crack model) on a transform fault versus time.

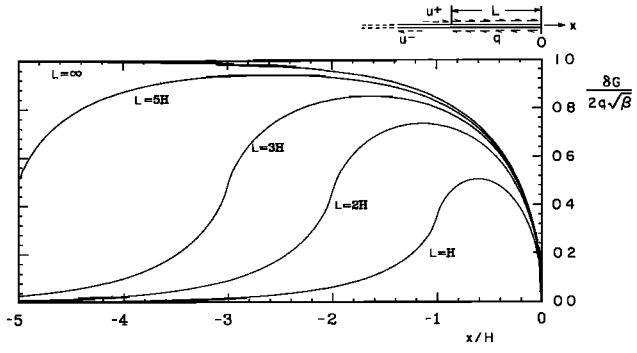


Fig. 6. Initial slip displacement associated with sudden stress drop $q$ on segment $L$ of semi-infinite strike slip fault.

An unrealistic feature is the $1/(x)^{1/2}$ singularity for the stress as $x \to 0^+$. This could be avoided through a more comprehensive constitutive modeling of the rupture process in the near-tip region of the crack, i.e., by introducing a 'break-down zone' in this region as in the work of *Palmer and Rice* [1973] and subsequent studies based thereupon [e.g., *Rice,* 1980]. We emphasize again, however, that the theory employed in this paper is limited in scope to large scale phenomena and cannot be expected to yield accurate modeling of thickness-averaged quantities at distances from the rupture front (or 'crack tip') which are small in comparison with the thickness of the lithosphere. We shall thus focus on the behavior of solutions at distances typically of the order of $H$ ahead of or behind the rupture front, i.e., beyond the unrealistic stress concentrations resulting from the crack tip singularity. A valid measure of the stress concentration arising near the edge of a zone of permanent stress drop will be the thickness-averaged Mode II stress intensity factor as given by (44) and plotted in Figure 5 versus dimensionless time for a uniform stress drop and different ratios of rupture length to lithosphere thickness. The dependence of this stress intensity factor on rupture length is seen to be quite marked, and so is the difference between its initial and final values (47) and (48), which, for the longer ruptures, reveals a very significant effect of load transfer from the relaxing asthenosphere to the lithosphere. However, the rise of $K$ with time is likely to be exaggerated, as is the time-dependent stress alteration in Figure 4, both reflecting the extreme condition of a permanent drop in stress along the rupture.

The sequence of figures just discussed was prepared for the strike-slip (or transform) mode. By using the transformation noted earlier to the thrust mode, as appropriate for a gently dipping fault plane, identical results apply to that case but with $\sigma_{xy}$ replaced by $\sigma_{yy}$, with the surface rupture lengths

$$L/H = 0,\ 1,\ 2,\ 3,\ 5,\ \infty$$

of various illustrations replaced by the sequence

$$L/H = 0,\ 0.61,\ 1.22,\ 1.83,\ 3.05,\ \infty$$

and with the distance marks

$$x/H = 0,\ 1,\ 2,\ 3,\ \cdots$$

on the horizontal axis in Figure 4 (and equally in Figures 6, 7, and 9) replaced by

$$x/H = 0,\ 0.61,\ 1.22,\ 1.83,\ \cdots$$

A time-varying slip movement is predicted to occur along the fault in response to a suddenly introduced rupture accompanied by a permanent stress drop. Postseismic slippage will however be hindered in reality by time-dependent strengthening of the fault and is therefore likely to be exaggerated by the crack model. Nevertheless, the amount of coseismic slippage is of considerable interest and, in the model considered next, can well serve as what would seem a reasonably realistic initial condition for a dislocation-type fault model. We therefore return to (36) and (30) from which the Laplace transform for the slip displacement along the fault is derived in Appendix C. For the short time limit $t \to 0^+$ ($\lambda \to \lambda_0$) we deduce from (C7) the following expression for the initial slip displacement due to a finite zone of stress drop:

$$\delta(x, 0^+) = \frac{2q}{G}\left(\frac{\beta}{\pi}\right)^{1/2} \int_0^{\lambda_0|x|} \frac{e^{-\rho}}{\rho^{1/2}} \operatorname{erf}\{[\rho + \lambda_0(L - |x|)]^{1/2}\}\, d\rho \qquad -L \le x \le 0 \tag{50}$$

$$\delta(x, 0^+) = \frac{2q}{G}\left(\frac{\beta}{\pi}\right)^{1/2} \int_{\lambda_0(|x|-L)}^{\lambda_0|x|} \frac{e^{-\rho}}{\rho^{1/2}} \operatorname{erf}\{[\rho - \lambda_0(|x| - L)]^{1/2}\}\, d\rho \qquad x < -L$$

A plot of this relation in dimensionless form is shown in Figure 6 where $\lambda_0 L$ has again been replaced by $L/H$, ranging from 1 to $\infty$. The simple result for $L \to \infty$ is

$$\delta(x, 0^+) = \frac{2q\beta^{1/2}}{G} \operatorname{erf}[(\lambda_0|x|)^{1/2}] \tag{51}$$

which shows that the initial slip displacement along a long rupture lies less than 5% below its maximum value of $2q\beta^{1/2}/G$ at $\lambda_0|x| \approx 2$ or larger, this maximum being identical with the initial slip displacement along an infinite fault which experiences a sudden stress drop [*Rice,* 1980]. It is interesting to compute the maximum mean slip displacement predicted by our model for a thickness averaged stress drop of 50 bar, say. Taking $\nu = 0.25$, $\beta^{1/2}(1 + \nu) = \lambda_0^{-1} \approx 75$ km and $G = 5.5 \times 10^{10}$ Pa, we find $\delta_{max} \approx 11$ m, which fits well into the range of observed slip displacements for great earthquakes.

*The Suddenly Introduced Dislocation Distribution*

The intended use of (50) is as an initial condition in modeling a suddenly introduced rupture in which post-seismic slip is prevented by a rapid restrengthening of the fault zone, the nature of which we shall leave open here. In this dislocation-type fault model the subsidiary conditions associated with (11) are the following:

$$u(x, 0^+, t) = \frac{1}{2}\delta(x)H(t) \qquad x < 0$$
$$u(x, 0^+, t) = 0 \qquad x > 0 \tag{52}$$

presupposing, in addition, an appropriate behavior of $u$ at large distances from the crack-tip. In the above $\delta(x)$ denotes the slip distribution as defined by (12) and produced initially by a constant stress drop rupture event, i.e., $\delta(x)$ is the function given by (50) and plotted in Figure 6.

The Fourier inversion of (18), making use of the convolution theorem and a table of integrals, gives

$$\hat{\sigma}_{xy}(x, 0, s) = \frac{(1 + \nu)G\lambda}{2\pi s} \int_{-\infty}^{0} K_1(|x - \xi|\lambda) \frac{\delta(\xi)\, d\xi}{|x - \xi|} \tag{53}$$

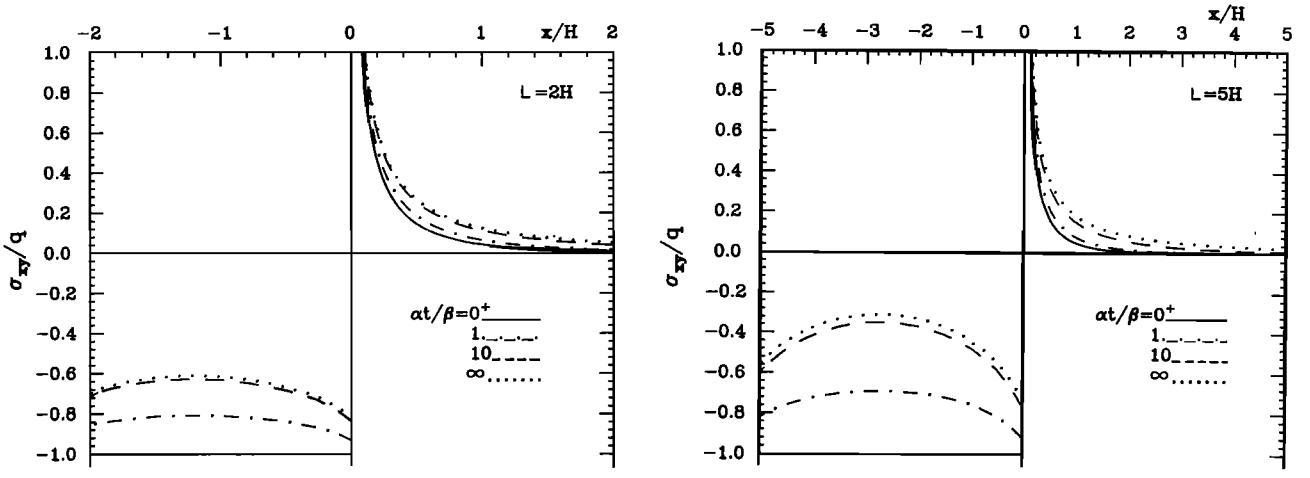


Fig. 7. Stress alteration for dislocation model of strike slip fault on and ahead of rupture zone at various times.

where $K_1$ is a modified Bessel function and for $x < 0$ the integral exists in the sense of its Cauchy principal value. The Laplace transform inversion of $(\lambda/s)K_1(|x - \xi|\lambda)$ is outlined in Appendix C. The result is

$$\sigma_{xy}(x, 0, t) = \frac{(1 + \nu)G}{2\pi} \int_{-\infty}^{0} \tau(|x - \xi|, t) \frac{\delta(\xi)\, d\xi}{|x - \xi|} \tag{54}$$

where

$$\tau(|x - \xi|, t) = \lambda_0 e^{-\alpha t/\beta} \left\{ K_1(|x - \xi|\lambda_0) + \sum_{\nu=1}^{\infty} \frac{(|x - \xi|\lambda_0 \alpha t/\beta)^\nu}{2^\nu(\nu!)^2} K_{\nu+1}(|x - \xi|\lambda_0) \right\}$$

The short time limit for $t \to 0$ may be verified to coincide with (45), as it should, when $\delta(x)$ is substituted from (50). Equation (54) for this slip distribution was evaluated by numerical integration and results are plotted in Figure 7 for different ratios of rupture length to lithosphere thickness and for multiples of the relaxation time $\beta/\alpha$, again assuming $\nu = 0.25$ and $\lambda_0 \approx 1/H$. Figure 7 affords a comparison with the crack solution of Figure 4 for points $x > 0$ ahead of the crack tip, and for $-L < x < 0$ shows the stress alterations within the zone of initial stress drop due to stress transfer from the asthenosphere onto the locked rupture zone.

The distinguishing features of the dislocation solution are seen to be significant time-dependent stress changes in the rupture zone itself and comparatively smaller stress alterations beyond the rupture front. In comparing Figures 7*a* and 7*b* we see that larger ruptures produce greater postseismic stress alterations. For $L = 5H$ about 70% of the initial stress drop is eventually eliminated at the center of the rupture zone by asthenosphere relaxation, while for $L = 2H$ only about 40% is eliminated. Thus shorter ruptures exhibit larger permanent stress drops.

We also note that the approximate symmetry of the stress distribution within the rupture zone about the point $x = -L/2$ confirms that a semi-infinite zone of slippage and a finite zone will yield stress distributions on the rupture plane and ahead of it which are qualitatively in agreement and quantitatively close enough to justify our initial replacement, for mathematical convenience, of a finite fault by a semi-infinite fault (cf. Figure 3).

The rupture front or crack tip in Figure 7 is characterized by a sharp transition from the stress minimum, which at finite times appears near the end of the slipping region, to the stress concentration which is encountered upon approaching the rupture from outside. Although details will vary to some extent, the same qualitative stress pattern may be expected to persist for different initial slip distributions. It seems possible therefore that the low stress zone behind the rupture front may act as a barrier to future propagating ruptures, thus furnishing one explanation for the observed tendency of rupture zones (including aftershock areas) of successive great earthquakes to abut without appreciable overlap [e.g., *Fedotov*, 1965; *Mogi*, 1968*a*; *Sykes*, 1971]. Moreover, it is near stress concentrations of the type shown in Figure 7 that one would expect future ruptures to originate preferentially, to advance from there into the more highly strained region adjacent to the original rupture; this indeed appears to be an observed pattern [*Kelleher*, 1970; *Sykes*, 1971; *Kelleher and Savino*, 1975].

If one explains the time interval separating the occurrence of neighboring great earthquakes in terms of missing strain energy which must be supplied by further loading in time before a rupture can be extended, then it will be of interest to examine the contribution of stress transfer from a relaxing asthenosphere to this loading of regions bordering a new rupture. Clearly, if significant stress is transferred at high enough rates by this mechanism, triggering interactions of adjacent events may be expected, a consequence being perhaps the clustering in time of individual events into distinct rupture sequences followed by longer intervals of relative quiescence extending over a certain segment of a seismic belt. Relevant to this question will be a comparison of the relative rate of stress alteration $\dot{\sigma}_{xy}/q$ (or $\dot{\sigma}_{yy}/q$ for the thrust mode) with an average tectonic stress rate normalized in the same way by the stress drop. In fact, tectonic stress rate as well as stress drop are both taken appropriately as long time averages for a large number of earthquake cycles so that we may set the ratio of average tectonic stress rate to stress drop $q$ equal to $t_r^{-1}$, where $t_r$ is the recurrence time.

Figure 8 affords a comparison between stress alterations due to load transfer from a relaxing asthenosphere as implied by Figures 4 and 7, and tectonic stressing for values of $t_r$ commonly mentioned in the literature. Plotted are stress alteration versus real time, letting $\beta/\alpha = 5$ yr, for the crack as well as for

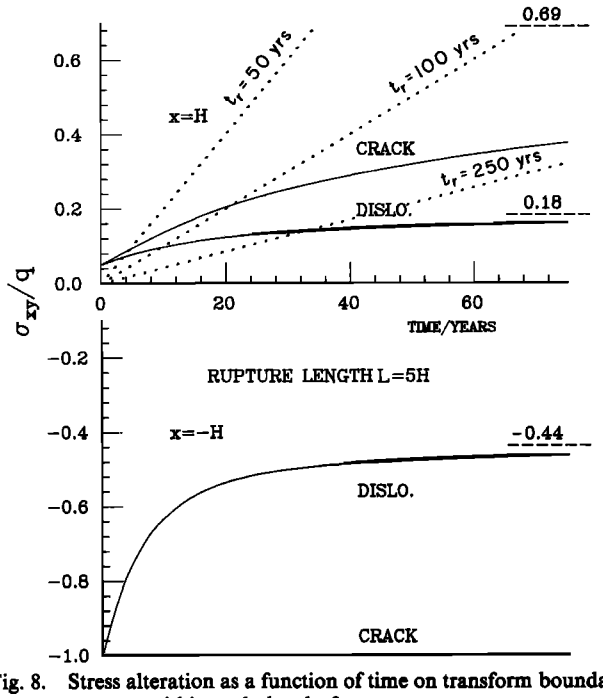


Fig. 8. Stress alteration as a function of time on transform boundary within and ahead of rupture zone.

the dislocation problem at distances of one lithosphere thickness ahead of and behind the rupture front, assuming a rupture length of five lithosphere thicknesses. The actual times associated with ordinates on the plots of Figure 8 increase or decrease in proportion to $\eta$ when $\eta$ differs from $2.0 \times 10^{19}$ Pa s. Also, for the thrust mode the equivalent rupture length is $L = 3H$. The stress alteration at $x = H$ is seen to increase slowly up to a saturation level amounting to 18% of the magnitude of the initial stress drop for the dislocation problem, but 69% of $q$ for the crack problem. As has been pointed out already, the crack solution is expected to predict unrealistically high stress changes while the dislocation solution will set a lower limit because it suppresses postseismic slip. Nevertheless, the latter is likely to be somewhat closer to reality.

The dotted lines in Figure 8 represent the accumulation of tectonic stress, expressed as a fraction of $q$, at a rate equal to $t_r^{-1}$ counted from the rupture event at $t = 0$. The supposition is now that at the time immediately after the rupture the stress at $x = H$ is increased by an instantaneous elastostatic alteration of about $0.05q$, but is still below the critical level at which a rupture can occur. The remaining necessary stress is then supplied by the added contributions of tectonic loading and load transfer from the relaxing asthenosphere. Assume now that the increase in stress still required at $x = H$ is some fraction of $q$, say $\frac{1}{2}q$, for example. This could be accomplished by tectonic loading alone at a rate of $t_r^{-1} = 1/100$ year within 50 years. Taking the lowest (dislocation solution) estimate for stressing due to asthenosphere relaxation and adding this to the tectonic loading rate one finds that the required additional load of $\frac{1}{2}q$ will be supplied in only 35 years. Although the magnitude of this acceleration effect depends somewhat on recurrence time, it remains significant within a range of 50 to 250 years which may be regarded as typical. This suggests that major and great earthquakes should occur in some concerted fashion determined by lithosphere/asthenosphere coupling effects. In fact, as a consequence of the acceleration mechanism implied by Figure 8 there should exist a tendency towards progressive synchronization of adjacent ruptures during repeated earthquake cycles.

Temporal clustering of large events has indeed been observed and, according to *Sykes et al.* [1980], who recently have examined the historical record for the Alaska-Aleutian arc, 'appears to be a common feature of several simple plate boundaries' including such examples as the plate boundary off northern Japan and the southern Kuril Islands and the North Anatolian fault. Disturbances of this clustering trend may result from material inhomogeneities and geometrical irregularities of the plate boundary and indeed, from Figure 8, the stress anomalies associated with such features need only be of the order of a few bars to put neighboring ruptures effectively out of phase.

From the lower half of Figure 8 it is apparent that according to the dislocation model the stress at $x = -H$, i.e., on the rupture zone itself, increases for a number of years at a much higher rate than it does on the adjacent plate boundary segment at $x = H$. This suggests an important role of asthenosphere relaxation in aftershock occurrence, taken in the broader sense of *Mogi* [1969] as prolonged anomalous seismic activity. Indeed, the shape of the stress isochrones on the rupture plane as it appears in Figure 7 is suggestive of a tendency towards more persistent long-term aftershock activity within a central section of the rupture zone. Beyond the rupture front, on the other hand, one may expect aftershock activity in the stricter sense associated with the stress concentration, but, owing to the lower stress rates, an even more prolonged seismic activity due to asthenosphere relaxation leading gradually into a concentration of long-term precursory events near the margin of the next great rupture. Such a behavior could resemble in certain aspects the 'seismic preconditions' noted by *Kelleher and Savino* [1975] as well as *Mogi*'s [1969] observation of long-term regularities in the space and time distribution of seismicity associated with certain great earthquakes. Although a more detailed prediction of such regularities will obviously require more sophisticated modeling, the results of our study indicate that lithosphere/asthenosphere coupling effects are likely to enter into the basic mechanism of any prolonged (i.e., of the order of a relaxation time) anomalous seismic activity preceding or following major or great ruptures.

## MIGRATING DISTURBANCES

In this section we explore the effects of lithosphere/asthenosphere coupling on the characteristics of propagating disturbances akin perhaps in certain basic aspects to propagating deformation fronts or triggering disturbances as have been discussed in connection with earthquake migration. To simplify the analysis, we focus on a large tectonic size scale and a long time scale and we shall model a 'deformation front' by a continuously propagating zone of permanent stress drop, i.e., by a steadily advancing crack. We shall thus deal with a variant of the preceding crack problem. In reality, of course, slip will often be discontinuous in time and distributed in space in the manner of shear zones in the upper crustal regions, but for the present purpose we average it out, analogously to the treatments by *Brune* [1968] and *Kostrov* [1973] of 'seismic flow' of rock masses over long time scales.

With reference to Figure 3*c* and the relevant discussion of the previous section, let the crack problem to be analyzed in the following consist of a similar Mode II crack advancing, however, steadily in positive $x$ direction at a fixed speed $V$. Subtracting out a remotely uniform tectonic stress $\tau_\infty$, we are led to the problem of a travelling crack subject to a follower load $-q(x - Vt) \equiv \tau_F(x - Vt) - \tau_\infty$ distributed over a segment

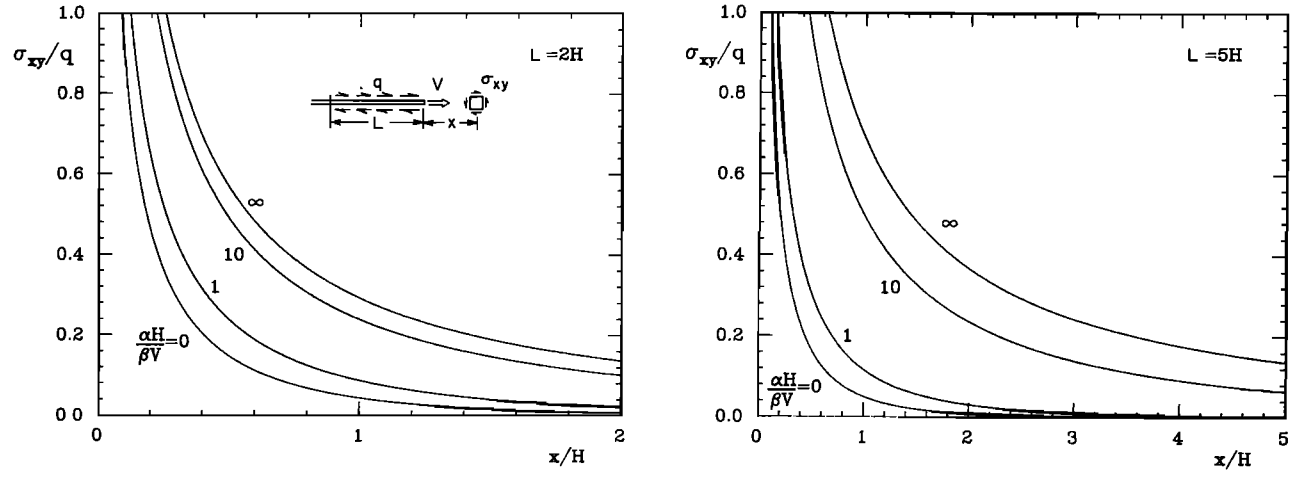


Fig. 9. Stress alteration along transform boundary ahead of travelling zone of uniform stress drop $q$ (propagating crack model) for various propagation speeds.

of length $L$ behind the crack tip. Mathematically this suggests a solution to (11) of the form

$$u(x, y, t) = u(x - Vt, y) \tag{55}$$

We therefore choose the origin of a new $x$, $y$ coordinate system at the tip of the travelling crack and shall thus deal with the following boundary value problem

$$(\alpha - \beta V\partial/\partial x)\,[(1 + \nu)^2\partial^2 u/\partial x^2 + \partial^2 u/\partial y^2] + V\partial u/\partial x = 0 \tag{56}$$

$$\begin{aligned} &u(x, 0) = 0 && x > 0 \\ &G\partial u/\partial y(x, 0) = -q(x) && x < 0 \\ &\partial u/\partial x,\ \partial u/\partial y \to 0 && x^2 + y^2 \to \infty \end{aligned} \tag{57}$$

Again, further conditions on the boundedness and decay of the displacement and its derivatives need to be assumed subsequently in order to ensure a solution. The method of solution closely parallels that employed for the transient crack problem of the previous section. Fourier transformation of (56) yields

$$(\alpha - \beta Vi\omega)\,[d^2\bar{u}/dy^2 - (1 + \nu)^2\omega^2\bar{u}] + Vi\omega\bar{u} = 0 \tag{58}$$

and restricting consideration to the half plane $y \geq 0$, the general solution of this equation is

$$\bar{u}(\omega, y) = A(\omega)e^{-(1+\nu)k(\omega)y} \qquad \text{Re}\,[k(\omega)] > 0 \tag{59}$$

where

$$k(\omega) = (\omega)^{1/2}(\omega - ia)^{1/2}(\omega + ib)^{1/2}(\omega + ic)^{-1/2} \tag{60}$$

and

$$\begin{aligned} a = a(V) &= \frac{1}{2}\,\{[(\alpha/\beta V)^2 + 4/\beta(1 + \nu)^2]^{1/2} - (\alpha/\beta V)\} \\ b = b(V) &= \frac{1}{2}\,\{[(\alpha/\beta V)^2 + 4/\beta(1 + \nu)^2]^{1/2} + (\alpha/\beta V)\} \\ c = c(V) &= \alpha/\beta V \end{aligned} \tag{61}$$

Clearly, $a$, $b$, and $c$ are positive real functions of $V$. Accordingly, in order to meet the requirement Re $[k(\omega)] > 0$, the branch cuts of $k(\omega)$ must be properly selected.

An application of the Wiener-Hopf technique which closely parallels the developments of Appendix B and the previous section now leads to the following results for the transformed displacement and stress along the $x$ axis:

$$(1 + \nu)G\bar{u}(\omega, 0^+) = \frac{i}{2\pi}\int_{-\infty - i\delta}^{+\infty - i\delta} \frac{Q(\kappa)\,d\kappa}{(\omega - \kappa)k_+(\omega)k_-(\kappa)} \tag{62}$$

and

$$\bar{\sigma}_{xy}(\omega, 0) = -\frac{i}{2\pi}\int_{-\infty - i\delta}^{+\infty - i\delta} \frac{Q(\kappa)k_-(\omega)\,d\kappa}{(\omega - \kappa)k_-(\kappa)} \tag{63}$$

where

$$\begin{aligned} k_+(\omega) &= (\omega)^{1/2}(\omega + ib)^{1/2}(\omega + ic)^{-1/2} \\ k_-(\omega) &= (\omega - ia)^{1/2} \end{aligned} \tag{64}$$

and $Q(\kappa)$ is again the transform of the load $q(x)$ as defined by (35).

A comparison with (37) now shows that the stress may be obtained from (63) by Fourier synthesis without further effort upon reinterpreting terms in (40), i.e., replacing $\lambda(s)$ by $a(V)$ and deleting the transform variable $s$. The result is

$$\sigma_{xy}(x, 0) = \frac{1}{\pi x^{1/2}}\int_{-\infty}^{0} q(\xi)\,\frac{(-\xi)^{1/2}}{x - \xi}\,e^{-a(V)(x-\xi)}\,d\xi \qquad x > 0 \tag{65}$$

Similarly, from (41) we deduce the expression

$$K(V) = \left[\frac{2}{\pi}\right]^{1/2}\int_{-\infty}^{0} q(\xi)\,\frac{e^{a(V)\xi}}{(-\xi)^{1/2}}\,d\xi \tag{66}$$

for the stress intensity factor. When a uniform stress drop $q$ occurs over $-L \leq x \leq 0$, in which case the lower limit in (65) and (66) is to be replaced by $-L$, the last result becomes

$$K(V) = q[2/a(V)]^{1/2}\,\text{erf}\,\{[a(V)L]^{1/2}\} \tag{67}$$

For unbounded $L$ and non-zero $V$ (66) yields

$$K(V) = q[2/a(V)]^{1/2} \tag{68}$$

In this special case integration of (65) also furnishes the result

$$\sigma_{xy}(x, 0) = q\,\{[1/(\pi a(V)x)^{1/2}]e^{-a(V)x} - \text{erfc}\,[(a(V)x)^{1/2}]\} \qquad x > 0 \tag{69}$$

Figures 9 and 10 present graphs of these solutions for uniform $q$ and various ratios of rupture length to lithosphere thickness, based again on the choices $\nu = 0.25$ and $(1 + \nu)\beta^{1/2} \approx H$. Note that the velocity parameter $\alpha(1 + \nu)/\beta^{1/2}\,V$ appear-

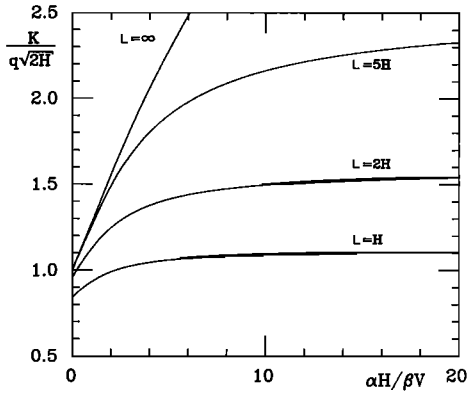


Fig. 10. Thickness average stress intensity factor associated with travelling zone of uniform stress drop on a transform fault versus 'slowness' of propagation.

ing in $a(V)$ may then be written as $\alpha H/\beta V$. Accordingly, in preparing Figures 9 and 10, we have used the expression

$$a(V) \approx \tfrac{1}{2}\{[(\alpha H/\beta V)^2 + 4]^{1/2} - (\alpha H/\beta V)\}/H \qquad (70)$$

These results for the stress distribution ahead of the crack and for the associated stress intensity factors display a dependence on the propagation speed of the crack through the parameter $a$. The function $a(V)$, as given by (61), is seen to approach the values $2V/[\alpha(1 + \nu)^2]$ and $1/[\beta^{1/2}(1 + \nu)]$ at low and high speeds, respectively. For the particular choice (70) the same limits are $2\beta V/\alpha H^2$ and $1/H$, respectively, and these have a simple interpretation in terms of the relative magnitude of an effective travel time $H/V$ and the relaxation time $\beta/\alpha$. The low-speed asymptote characterizes purely viscous response of the asthenosphere, as in Elsasser's model, while in the high-speed limit there remains no time for viscous relaxation and the asthenosphere responds elastically. As is to be expected, in the high-speed limit the solution for the travelling crack reproduces the short-time limit (45) of the transient crack problem of the previous section, the same being true, of course, for the stress intensity factor. On the other hand, $a(V \to 0) = 0$ so that for any finite $L$ the elastic solutions (46) and (48) are again recovered, and it is clear indeed that the limits $V \to 0$ for the travelling crack and $t \to \infty$ for the stationary crack are equivalent in that the asthenosphere will become completely relaxed in each case, thus leading to identical solutions for a freely floating elastic plate.

The fact that $a(V)$ increases monotonically has the important consequence that the stress ahead of the crack as well as the stress intensity factor become more strongly attenuated the higher the propagation speed $V$ and hence the greater the elastic load-carrying capacity of the asthenosphere. This coupling effect is quite analogous to one displayed by a simple rheological model consisting of a spring (lithosphere) and a Maxwell element (asthenosphere) in parallel arrangement. In such a model the distribution of the total load over both elements is determined by the rate of loading, just as in our model the load distribution over asthenosphere and lithosphere depends on the propagation speed of the zone of stress drop.

Figures 9 and 10 permit a quick assessment of the role of lithosphere/asthenosphere coupling effects for a given propagation speed of a zone of reduced stress. Taking $\beta/\alpha = 5$ yr, $H = 75$ km and $V = 100$ km/yr as a typical order of magnitude, we find that $\alpha H/\beta V = 0.15$. Hence, for migration speeds of 100 km/yr or higher, the asthenosphere is virtually unrelaxed and the zone of stress drop propagates as if over an elastic foundation, led by significantly reduced stresses and stress concentrations. Any sizeable reduction in $V$ from 100 km/yr will imply a load transfer from the asthenosphere to the lithosphere, on the other hand, which can be read off Figures 9 and 10, and this may lead into an earthquake instability. Indeed, in the extreme case of arrest of a disturbance propagating previously at a speed of the order of 100 km/yr or larger, the process analyzed in the previous section will evolve, enabling the arrested disturbance to shed gradually significant stress on any barrier and thereby to trigger a delayed rupture.

## CONCLUDING DISCUSSION

The preceding analysis seeks to provide a model for large-scale stress and strain diffusion phenomena in a lithospheric plate, reflecting dynamic coupling of the latter to a viscoelastic asthenospheric substrate. In contrast with *Elsasser*'s [1969] theory of lithospheric stress guides, in which a purely viscous asthenosphere and very long (spatial) wavelength disturbances are assumed, our model is able to deal with sudden events such as earthquake faulting along a limited plate boundary segment. The theory presented is general enough, for example, to serve as a basis for modeling large scale in-plane deformations and stresses associated with a variety of tectonophysical phenomena affecting the lithosphere, such as major volcanic eruptions or intrusive processes of the type occurring at spreading centers. Also, certain phenomena of stress and strain diffusion from the boundaries into the interior of plates that have been linked to the occurrence of intraplate earthquakes [*Shimazaki,* 1978; *Ishii et al.,* 1978; *Yamashina,* 1979; *Seno,* 1979] appear to lie within the scope of our theory.

A principal limitation of any plate theory lies of course in its two-dimensional nature which implies an averaging over any depth variation and forces us, in particular, to disregard the details of processes at plate boundaries. Nevertheless, it would seem feasible in future more comprehensive modeling to employ suitable matching techniques and thereby link the theoretical results obtained in this paper to detailed cross-sectional studies of rupture progression across the plate thickness so as to gain more complete insight into the role played by lithosphere/asthenosphere coupling.

From the solutions obtained in this paper and illustrated by Figures 4–10 the following main conclusions may be drawn: The stress which is shed by a great earthquake onto the asthenosphere is gradually transferred back to the lithosphere by a relaxation process. Accordingly, postseismic increases in stress will be felt outside the rupture zone, which may exceed coseismic elastostatic stress alterations several times and amount in magnitude to an appreciable fraction of the stress drop on the fault at a distance of one lithosphere thickness away from the rupture front. When postseismic slippage along the fault is unimportant, the stress on the fault will build up in time due to the same mechanism of asthenosphere relaxation. The spatial and temporal characteristics of this postseismic stressing, as illustrated in Figures 7 and 8, are quite distinct for points located on the rupture and beyond it and suggest characteristic patterns of prolonged aftershock activity for locations inside and outside a new rupture zone. Quite generally, stress diffusion away from great ruptures implies a tendency towards progressive synchronization of neighboring

events, a trend which is easily upset, however, by heterogeneities and geometrical irregularities (see discussion in connection with Figure 8).

When modeling migration of seismic activity along a plate boundary by a steadily advancing zone of stress drop, the altered stress state propagating ahead of this zone is found to correspond very closely to an essentially unrelaxed state of the asthenosphere at typical propagation speeds of 100 km/yr. When arrested by a barrier, a disturbance of this kind can transfer significant stresses to the barrier from a then relaxing asthenosphere and could thus act as a delayed trigger of a barrier breaking event.

## Appendix A: Solution to the General Model for Stresses Along a Plate Boundary Associated With an Arbitrary Slip Distribution

Here we develop the solution for the general model of (7) analogous to that presented for the simple model of (11) in (16)–(19). The displacements may be written as

$$u_x = \partial\phi/\partial x + \partial\psi/\partial y$$
$$u_y = \partial\phi/\partial y - \partial\psi/\partial x \tag{A1}$$

where the potentials are found to satisfy

$$(\alpha + \beta\partial/\partial t)\nabla^2\phi = [(1-\nu)/2]\partial\phi/\partial t$$
$$(\alpha + \beta\partial/\partial t)\nabla^2\psi = \partial\psi/\partial t \tag{A2}$$

(compare equations (9)). Taking Fourier and Laplace transforms as in (15) the solutions are, for $y > 0$,

$$\hat{\tilde{\phi}} = Ae^{-my} \qquad m = [\omega^2 + \tfrac{1}{2}(1-\nu)s/(\alpha+\beta s)]^{1/2}$$
$$\hat{\tilde{\psi}} = Be^{-ny} \qquad n = [\omega^2 + s/(\alpha+\beta s)]^{1/2} \tag{A3}$$

Boundary conditions to be satisfied on $y = 0$ are

$$u_x(x, y=0^+, t) - u_x(x, y=0^-, t) = 2u_x(x, y=0^+, t) = \delta(x, t)$$
$$\sigma_{yy}(x, 0, t) = 0 \tag{A4}$$

The latter condition follows from the complete anti-symmetry of the problem and, by the stress-strain relations of (2), it is equivalent to

$$\frac{\partial u_y}{\partial y}(x, y=0^+, t) + \nu\,\frac{\partial u_x}{\partial x}(x, y=0^+, t) = 0 \tag{A5}$$

Hence, using (A3), $A$ and $B$ are found to satisfy

$$2i\omega A - 2nB = \hat{\tilde{\delta}}$$
$$(m^2 - \nu\omega^2)A + i(1-\nu)\omega nB = 0 \tag{A6}$$

When these equations are solved for $A$ and $B$, and the relation

$$\sigma_{xy} = G(\partial u_y/\partial x + \partial u_x/\partial y) \tag{A7}$$

is used, we find that the transformed shear stress $\hat{\tilde{\sigma}}_{xy}$ on $y = 0$ is given by (18) with $S$ given by the expression in (20).

## Appendix B: Solution of (40) by the Wiener-Hopf Method

We wish to solve first for the particular case of the complex periodic load $q(x) = e^{i\kappa x}$, where $\kappa$ has a small negative imaginary part $-\delta$. From (32) there follows

$$Q(\omega) = -i/(\kappa - \omega) \tag{B1}$$

and (34) takes the special form

$$(1+\nu)G(\omega^2+\lambda^2)^{1/2}U_+^{(\kappa)}(\omega, s) = i/[s(\omega-\kappa)] - \hat{T}_-^{(\kappa)}(\omega, s) \tag{B2}$$

To solve this by the Wiener-Hopf method, we factorize the function $k(\omega) \equiv (\omega^2+\lambda^2)^{1/2}$ in the form

$$k(\omega) = k_+(\omega)k_-(\omega) \tag{B3}$$

choosing

$$k_+(\omega) = (\omega + i\lambda)^{1/2}$$
$$k_-(\omega) = (\omega - i\lambda)^{1/2} \tag{B4}$$

so that $k_+(\omega)$ is analytic in Im $(\omega) < \lambda$, the branch cuts in the $\omega$ plane being taken symmetrically along the imaginary axis. We now rearrange (B2) and write

$$(1+\nu)Gk_+(\omega)\hat{U}_+^{(\kappa)}(\omega, s) - i/[s(\omega-\kappa)k_-(\kappa)]$$
$$= i[1/k_-(\omega) - 1/k_-(\kappa)]/[s(\omega-\kappa)] - \hat{T}_-^{(\kappa)}(\omega, s)/k_-(\omega) \tag{B5}$$

This equality holds in the strip $0 < \text{Im}\,(\omega) < \tau \le \lambda$. With the functions on its left side analytic in Im $(\omega) > 0$ and that on its right side analytic in Im $(\omega) < \tau$, it follows that each function represent an analytic continuation of the other and therefore either side of (B5) may be set equal to one and the same entire function $E(\omega)$. Moreover, both $\hat{U}_+^{(\kappa)}(\omega, s)$ and $\hat{T}_-^{(\kappa)}(\omega, s)$ approach zero as $|\omega| \to \infty$ in their domain of analyticity. Therefore, by Liouville's theorem, the function $E(\omega)$ must vanish everywhere. Equating accordingly each side of (B5) to $E(\omega) \equiv 0$, one arrives at

$$(1+\nu)G\hat{U}_+^{(\kappa)}(\omega, s) = i/[s(\omega-\kappa)(\omega+i\lambda)^{1/2}(\kappa-i\lambda)^{1/2}] \tag{B6}$$

$$\hat{T}_-^{(\kappa)}(\omega, s) = i[1 - (\omega-i\lambda)^{1/2}(\kappa-i\lambda)^{-1/2}]/[s(\omega-\kappa)] \tag{B7}$$

## Appendix C: Solution of Some Inversion Problems

### 1. *Laplace Transform Inversion of* $(1/s)e^{-(r+x)\lambda(s)}$

We use theorem XII of *Carslaw and Jaeger* [1948, p. 259] stating that if $\hat{f}(s)$ and $\hat{\phi}(x, \eta)$ are Laplace transforms of $f(t)$ and $\phi(t, \eta)$, where $\hat{\phi}(x, \eta) = g(s)\exp[-\eta h(s)]$, then

$$\mathcal{L}^{-1}\{g(s)\hat{f}[h(s)]\} = \int_0^\infty \phi(t, \eta)f(\eta)\,d\eta$$

Let us apply this theorem to the transform

$$\frac{1}{s}\exp\{-\xi[s/(1+s)]^{1/2}\}$$

This will yield the inversion of the original transform upon replacing $t$ by $\alpha t/\beta$ and $\xi$ by $(r+x)\lambda_0$ in the final result. Take now

$$\hat{f}(s) = \frac{1}{s}e^{-\xi s^{1/2}} \qquad g(s) = \frac{1}{s} \qquad h(s) = \frac{s-1}{s}$$

Then

$$g(s)\hat{f}[h(s)] = \frac{1}{s-1}\exp\{-\xi[(s-1)/s]^{1/2}\} \equiv \hat{B}(\xi, s-1)$$

say. Also

$$\hat{\phi}(s, \eta) = \frac{1}{s}\exp[-\eta(s-1)/s] = \frac{1}{s}e^{-\eta}e^{\eta/s}$$

Now, by the shifting theorem $\mathscr{L}^{-1}\{\hat{B}(\xi, s-1)\} = e^t B(\xi, t)$, so that

$$B(\xi, t) \equiv \mathscr{L}^{-1}\left\{\frac{1}{s}\exp\left[-\xi(s/(1+s))^{1/2}\right]\right\} = e^{-t}\mathscr{L}^{-1}\{g(s)\hat{f}[h(s)]\}$$

From a table of transforms we obtain $f(t) = \operatorname{erfc}[\xi/(2t^{1/2})]$ and $\phi(t, \eta) = e^{-\eta}I_0[2(\eta t)^{1/2}]$. By the above theorem, therefore

$$\mathscr{L}^{-1}\left\{\frac{1}{s}\exp\left[-\xi(s/(1+s))^{1/2}\right]\right\} = e^{-t}\int_0^\infty e^{-\eta}\operatorname{erfc}[\xi/(2\eta^{1/2})]I_0[2(\eta t)^{1/2}]\,d\eta \tag{C1}$$

Replacing $t$ by $\alpha t/\beta$ and $\xi$ by $(r + x)\lambda_0$, one thus obtains (43) and similarly (44).

*2. Laplace Transform Inversion of $(1/s)\lambda(s)K_1[|x-\xi|\lambda(s)]$*

Consider the inversion of

$$\frac{1}{s}\left(\frac{s}{1+s}\right)^{1/2}K_1\left[\xi\left(\frac{s}{1+s}\right)^{1/2}\right]$$

We apply the same method as in the above, selecting

$$\hat{f}(s) = \frac{1}{s^{1/2}}K_1(s^{1/2}) \qquad g(s) = \frac{1}{s} \qquad h(s) = (s-1)/s$$

This gives

$$g(s)\hat{f}[h(s)] = \frac{1}{s-1}\left(\frac{s-1}{s}\right)^{1/2}K_1\left[\xi\left(\frac{s-1}{s}\right)^{1/2}\right]$$

and

$$f(t) = \frac{1}{\xi}e^{-\xi^2/4t}$$

from a table. Going through identical steps again, while noticing that $\phi(t, \eta)$ remains the same as under Appendix C1, we get

$$\mathscr{L}^{-1}\left\{\frac{1}{s}\left(\frac{s}{1+s}\right)^{1/2}K_1\left[\xi\left(\frac{s}{1+s}\right)^{1/2}\right]\right\} = \frac{1}{\xi}e^{-t}\int_0^\infty \exp(-\eta - \xi^2/4\eta)I_0[2(\eta t)^{1/2}]\,d\eta$$

$$= e^{-t}\left\{K_1(\xi) + \sum_{\nu=1}^{\infty}\frac{(\xi t)^\nu}{2^\nu(\nu!)^2}K_{\nu+1}(\xi)\right\} \tag{C2}$$

To obtain the last expression, use has been made of the series representation $I_0(z) = \sum_{\nu=0}^{\infty}(z/2)^{2\nu}/(\nu!)^2$ and an integral representation for $K_\nu$. Taking care now of a factor $\lambda_0$ by which the original transform differs from the one inverted here and replacing $\xi$ and $t$ by $|x-\xi|\lambda_0$ and $\alpha t/\beta$, respectively, one arrives at (54).

*3. Fourier Inversion of Slip Displacement Along Suddenly Introduced Crack*

By virtue of (30), relation (B6) furnishes the Fourier-Laplace transform of the slip displacement along a semi-infinite crack subject to a suddenly introduced elementary load $q(x) = e^{i\kappa x}$, $x < 0$, and further conditions specified by (29). The same method of superposition which was applied in deriving relation (38) now enables us to write down a solution $\hat{U}_+(\omega, s)$ to (34) for a general loading $q(x)$ in the form

$$\hat{U}_+(\omega, s) = \frac{1}{2\pi}\int_{-\infty-i\delta}^{+\infty-i\delta}\hat{U}_+^{(\kappa)}Q(\kappa)\,d\kappa \tag{C3}$$

where $\hat{U}_+^{(\kappa)}$ is the elementary solution given by (B6) and $Q(\kappa)$ is the Fourier transform of the actual load, as defined by (35). Thus

$$\hat{U}_+(\omega, s) = \frac{i}{2\pi(1+\nu)Gs}\int_{-\infty}^0 q(\xi)\,d\xi \cdot \int_{-\infty-i\delta}^{+\infty-i\delta}\frac{e^{-i\kappa\xi}\,d\kappa}{(\omega-\kappa)(\omega+i\lambda)^{1/2}(\kappa-i\lambda)^{1/2}} \tag{C4}$$

and after a formal Fourier inversion

$$\hat{u}(x, 0^+, s) = \frac{i}{4\pi^2(1+\nu)Gs}\int_{-\infty}^0 q(\xi)\,d\xi \int_{-\infty-i\delta}^{+\infty-i\delta}d\kappa \cdot \int_{-\infty}^{\infty}\frac{e^{-i(\kappa\xi-\omega x)}\,d\omega}{(\omega-\kappa)(\omega+i\lambda)^{1/2}(\kappa-i\lambda)^{1/2}} \tag{C5}$$

Choosing integration contours along the branch cuts and evaluating the residue at the pole $\omega = \kappa$, we get

$$\hat{u}(x, 0^+, s) = \frac{1}{\pi(1+\nu)Gs}\int_{-\infty}^0 q(\xi)[I_1(x, \xi, s) - I_2(x, \xi, s)]\,d\xi \tag{C6}$$

where $I_1(x, \xi, s)$ and $I_2(x, \xi, s)$ are integrals still to be evaluated. We have

$$I_1 \equiv \int_\lambda^\infty \frac{e^{-\tau|x-\xi|}\,d\tau}{(\tau^2-\lambda^2)^{1/2}} = e^{\lambda(x+\xi)}\int_\alpha^\infty \frac{e^{-2\lambda\rho}\,d\rho}{(\rho-x)^{1/2}(\rho-\xi)^{1/2}} \qquad \alpha = \max(x, \xi)$$

and

$$I_2 \equiv \frac{1}{\pi}\int_\lambda^\infty\int_\lambda^\infty \frac{e^{\sigma x+\tau\xi}\,d\sigma\,d\tau}{(\sigma+\tau)(\sigma-\lambda)^{1/2}(\tau-\lambda)^{1/2}} = \int_\lambda^\infty \operatorname{erfc}\{[(\tau+\lambda)|x|]^{1/2}\}\frac{e^{-\tau(x-\xi)}\,d\tau}{(\tau^2-\lambda^2)^{1/2}} = e^{\lambda(x+\xi)}\int_0^\infty \frac{e^{-2\lambda\rho}\,d\rho}{(\rho-x)^{1/2}(\rho-\xi)^{1/2}}$$

after some manipulation involving the use of an integral representation for erfc. Substitution of these results in the above expression for $\hat{u}(x, 0^+, s)$ now yields

$$\hat{u}(x, 0^+, s) = \frac{1}{\pi(1+\nu)Gs}\left\{\int_{-\infty}^x q(\xi)e^{\lambda(x+\xi)} \cdot \int_x^0 \frac{e^{-2\lambda\rho}\,d\rho}{(\rho-x)^{1/2}(\rho-\xi)^{1/2}}\,d\xi + \int_x^0 q(\xi)e^{\lambda(x+\xi)} \cdot \int_\xi^0 \frac{e^{-2\lambda\rho}\,d\rho}{(\rho-x)^{1/2}(\rho-\xi)^{1/2}}\,d\xi\right\} \tag{C7}$$

We are interested in the case in which a stress drop occurs on a segment of length $L$ of the fault. The desired expression (50) for the initial slip displacement then follows from the general result (C7) upon letting $\lambda \to 1/[\beta^{1/2}(1+\nu)] = \lambda_0$ and ensuring proper limits of integration.

*Acknowledgments.* This research was supported by the National Science Foundation Geophysics Program and the U.S. Geological Survey Earthquake Hazards Reduction Program. We are grateful to D. A. Simons for discussions of mathematical techniques.

## REFERENCES


Ambraseys, N. M., Some characteristic features of the Anatolian fault zone, *Tectonophysics, 9,* 143–165, 1970.

Anderson, D. L., Accelerated plate tectonics, *Science, 187,* 1077–1079, 1975.

Bilby, B. A., and J. D. Eshelby, Dislocations and the theory of fracture, in *Fracture: An Advanced Treatise,* vol. 1, edited by H. Liebowitz, pp. 100–182, Academic, New York, 1968.

Bott, M. H. P., and D. S. Dean, Stress diffusion from plate boundaries, *Nature, 243,* 339–341, 1973.

Brune, J. N., Seismic moment, seismicity, and rate of slip along major fault zones, *J. Geophys. Res., 73,* 777–784, 1968.

Brune, J. N., Implications of earthquake triggering and rupture propagation for earthquake prediction based on premonitory phenomena, *J. Geophys. Res., 84,* 2195–2198, 1979.

Budiansky, B., and C. Amazigo, Interaction of fault slip and lithosphere creep, *J. Geophys. Res., 81,* 4897–4900, 1976.

Carslaw, H. S., and J. C. Jaeger, *Operational Methods in Applied Mathematics,* 2nd ed., Oxford University Press, New York, 1948.

Delsemme, J., and A. T. Smith, Spectral analysis of earthquake migration in South America, *Pure Appl. Geophys., 117,* 1271–1285, 1979.

Dewey, J. W., Seismicity of Northern Anatolia, *Bull. Seismol. Soc. Am., 66,* 843–868, 1976.

Elsasser, W. M., Convection and stress propagation in the upper mantle, in *The Application of Modern Physics to the Earth and Planetary Interiors,* edited by S. K. Runcorn, pp. 223–246, Wiley-Interscience, New York, 1969.

Erdelyi, A., W. Magnus, F. Oberhettinger, and F. G. Tricomi, *Tables of Integral Transforms,* vol. 1, McGraw-Hill, New York, 1954.

Fedotov, S. A., Regularities of the distribution of strong earthquakes in Kamchatka, the Kurile Islands, and Northeastern Japan, *Tr. Inst. Phys. Earth Acad. Sci. USSR, 36,* 66–93, 1965.

Ida, Y., Slow-moving deformation pulses along tectonic faults, *Phys. Earth Planet. Interiors, 9,* 328–337, 1974.

Ishii, H., T. Sato, and A. Takagi, Characteristics of strain migration in the Northeastern Japanese arc (I)—Propagation characteristics, *Sci. Rep. Tohoku Univ. Ser. 5, 25,* 83–90, 1978.

Kelleher, J. A., Space-time seismicity of the Alaska-Aleutian seismic zone, *J. Geophys. Res., 75,* 5745–5756, 1970.

Kelleher, J. A., and J. Savino, Distribution of seismicity before large strike slip and thrust-type earthquakes, *J. Geophys. Res., 80,* 260–271, 1975.

Kostrov, B. V., Seismic moment, earthquake energy and seismic flow of rocks, *Publ. Inst. Geophys. Pol. Acad. Sci., 62,* 25–47, 1973.

Melosh, H. J., Nonlinear stress propagation in the Earth's upper mantle, *J. Geophys. Res., 81,* 5621–5632, 1976.

Mogi, K., Sequential occurrence of recent great earthquakes, *J. Phys. Earth, 16,* 30–36, 1968*a*.

Mogi, K., Migration of seismic activity, *Bull. Earthquake Res. Inst. Univ. Tokyo, 46,* 53–74, 1968*b*.

Mogi, K., Some features of recent seismic activity in and near Japan, 2, Activity before and after great earthquakes, *Bull. Earthquake Res. Inst. Univ. Tokyo, 47,* 395–417, 1969.

Noble, B., *Methods Based on the Wiener-Hopf Technique,* Pergamon, New York, 1958.

Nur, A., and G. Mavko, Post-seismic viscoelastic rebound, *Science, 183,* 204–206, 1974.

Palmer, A. C., and J. R. Rice, The growth of slip surfaces in the progressive failure of overconsolidated clay, *Proc. R. Soc. London Ser. A, 332,* 527–548, 1973.

Reid, H. F., Permanent displacements of the ground, in *The California Earthquake on April 18, 1906: Report of the State Earthquake Investigation Commission,* vol. 2, pp. 16–28, Carnegie Institution, Washington, D. C., 1910.

Rice, J. R., Mathematical analysis in the mechanics of fracture, in *Fracture: An Advanced Treatise,* vol. 2, edited by H. Liebowitz, pp. 191–311, Academic, New York, 1968.

Rice, J. R., The mechanics of earthquake rupture, in *Physics of the Earth's Interior,* edited by A. M. Dziewonski and E. Boschi, pp. 555–649, Italian Physical Society/North-Holland, Amsterdam, 1980.

Rice, J. R., and D. A. Simons, The stabilization of spreading shear faults by coupled deformation-diffusion effects in fluid-infiltrated porous materials, *J. Geophys. Res., 81,* 5322–5334, 1976.

Richter, C. F., *Elementary Seismology,* W. H. Freeman, San Francisco, Calif., 1958.

Rudnicki, J. W., Fracture mechanics applied to the Earth's crust, *Annu. Rev. Earth Planet. Sci., 8,* 489–525, 1980.

Savage, J. C., A theory of creep waves propagating along a transform fault, *J. Geophys. Res., 76,* 1954–1966, 1971.

Savage, J. C., and W. H. Prescott, Asthenosphere readjustment and the earthquake cycle, *J. Geophys. Res., 83,* 3369–3376, 1978*a*.

Savage, J. C., and W. H. Prescott, Comment on 'Nonlinear stress propagation in the Earth's upper mantle' by H. J. Melosh, *J. Geophys. Res., 83,* 5005–5007, 1978*b*.

Scholz, C. H., A physical interpretation of the Haicheng earthquake prediction, *Nature, 267,* 121–124, 1977.

Seno, T., Pattern of intraplate seismicity in southwest Japan before and after great interplate earthquakes, *Tectonophysics, 57,* 267–283, 1979.

Shimazaki, K., Correlation between intraplate seismicity and interplate earthquakes, *Bull. Seismol. Soc. Am., 68,* 181–192, 1978.

Spence, D. A., and D. L. Turcotte, Viscoelastic relaxation of cyclic displacements on the San Andreas Fault, *Proc. R. Soc. London Ser. A, 365,* 121–144, 1979.

Sykes, L. R., Aftershock zones of great earthquakes, seismicity gaps, and earthquake prediction for Alaska and the Aleutians, *J. Geophys. Res., 76,* 8021–8041, 1971.

Sykes, L. R., J. B. Kisslinger, L. House, J. N. Davis, and K. H. Jacob, Rupture zones of great earthquakes in the Alaska-Aleutian arc, 1794–1980, *Science, 210,* 1343–1345, 1980.

Thatcher, W., T. Matsuda, T. Kato, and J. B. Rundle, Lithospheric loading by the 1896 Riku-u earthquake, northern Japan: Implications for plate flexure and asthenospheric rheology, *J. Geophys. Res., 85,* 6429–6439, 1980.

Toksöz, M. N., A. F. Shakal, and A. J. Michael, Space-time migration of earthquakes along the North Anatolian fault zone and seismic gaps, *Pure Appl. Geophys., 117,* 1258–1270, 1979.

Turcotte, D. L., R. Y. Clancy, D. A. Spence, and F. H. Kulhawy, Mechanism for the accumulation and release of stress on the San Andreas Fault, *J. Geophys. Res., 84,* 2273–2282, 1979.

Walcott, R. I., Structure of the Earth from glacio-isostatic rebound, *Annu. Rev. Earth Planet. Sci., 1,* 15–37, 1973.

Wood, M. D., and S. S. Allen, Recurrence of seismic migrations along the Central California segment of the San Andreas fault system, *Nature, 244,* 213–215, 1973.

Wyss, M. (Ed.), Special Issue: Earthquake Prediction and Seismicity Patterns, *Pure Appl. Geophys., 117*(6), 1979.

Yamashina, K., A possible factor which triggers shallow intra-plate earthquakes, *Phys. Earth Planet. Interiors, 18,* 153–164, 1979.


(Received November 21, 1980;
accepted January 30, 1981.)